geosciences

MDPI

Article

Assessing the Multiple Impacts of Extreme Hurricanes in Southern New England, USA

David S. Ullman [1,*], Isaac Ginis [1], Wenrui Huang [2], Catherine Nowakowski [1], Xuanyu Chen [1] and Peter Stempel [3]

1 Graduate School of Oceanography, University of Rhode Island, 215 South Ferry Road, Narragansett, RI 02882, USA; iginis@uri.edu (I.G.); cnowakowski@my.uri.edu (C.N.); xychen@my.uri.edu (X.C.)
2 Civil and Environmental Engineering Department, Florida State University, Tallahassee, FL 32310, USA; whuang@eng.famu.fsu.edu
3 Rhode Island School of Design, Providence, RI 02903, USA; pstempel@risd.edu
* Correspondence: dullman@uri.edu; Tel.: +1-401-874-6138

Received: 14 May 2019; Accepted: 14 June 2019; Published: 19 June 2019

check for updates

Abstract: The southern New England coast of the United States is particularly vulnerable to land-falling hurricanes because of its east-west orientation. The impact of two major hurricanes on the city of Providence (Rhode Island, USA) during the middle decades of the 20th century spurred the construction of the Fox Point Hurricane Barrier (FPHB) to protect the city from storm surge flooding. Although the Rhode Island/Narragansett Bay area has not experienced a major hurricane for several decades, increased coastal development along with potentially increased hurricane activity associated with climate change motivates an assessment of the impacts of a major hurricane on the region. The ocean/estuary response to an extreme hurricane is simulated using a high-resolution implementation of the ADvanced CIRCulation (ADCIRC) model coupled to the Precipitation-Runoff Modeling System (PRMS). The storm surge response in ADCIRC is first verified with a simulation of a historical hurricane that made landfall in southern New England. The storm surge and the hydrological models are then forced with winds and rainfall from a hypothetical hurricane dubbed "Rhody", which has many of the characteristics of historical storms that have impacted the region. Rhody makes landfall just west of Narragansett Bay, and after passing north of the Bay, executes a loop to the east and the south before making a second landfall. Results are presented for three versions of Rhody, varying in the maximum wind speed at landfall. The storm surge resulting from the strongest Rhody version (weak Saffir–Simpson category five) during the first landfall exceeds 7 m in height in Providence at the north end of the Bay. This exceeds the height of the FPHB, resulting in flooding in Providence. A simulation including river inflow computed from the runoff model indicates that if the Barrier remains closed and its pumps fail (for example, because of a power outage or equipment failure), severe flooding occurs north of the FPHB due to impoundment of the river inflow. These results show that northern Narragansett Bay could be particularly vulnerable to both storm surge and rainfall-driven flooding, especially if the FPHB suffers a power outage. They also demonstrate that, for wind-driven storm surge alone under present sea level conditions, the FPHB will protect Providence for hurricanes less intense than category five.

Keywords: storm surge; wave modeling; river flooding; hurricane impacts; hurricane wind model

1. Introduction

Although the southern New England coast of the United States has experienced a number of extreme hurricanes since the arrival of European settlers, there have been none in recent years. A decade ago, the Federal Emergency Management Agency (FEMA) identified Southern New England as the "Achilles heel of the Northeast" because of its hurricane vulnerability. Thus, it is important for preparedness planners to be aware of the potential impacts of intense hurricanes on the infrastructure of the region so that evacuation and response plans can be developed.

During the 20th century, southern New England was impacted by two strong hurricanes—by the so-called 1938 Great New England Hurricane and, 16 years later, by Hurricane Carol in 1954. Both storms made landfall to the west of Narragansett Bay (NB) and thus caused severe impacts to the NB region, which was located to the right of the storm centers. Providence, located at the extreme northern end of NB (Figure 1b), experienced severe flooding from storm surge during both of these hurricanes.

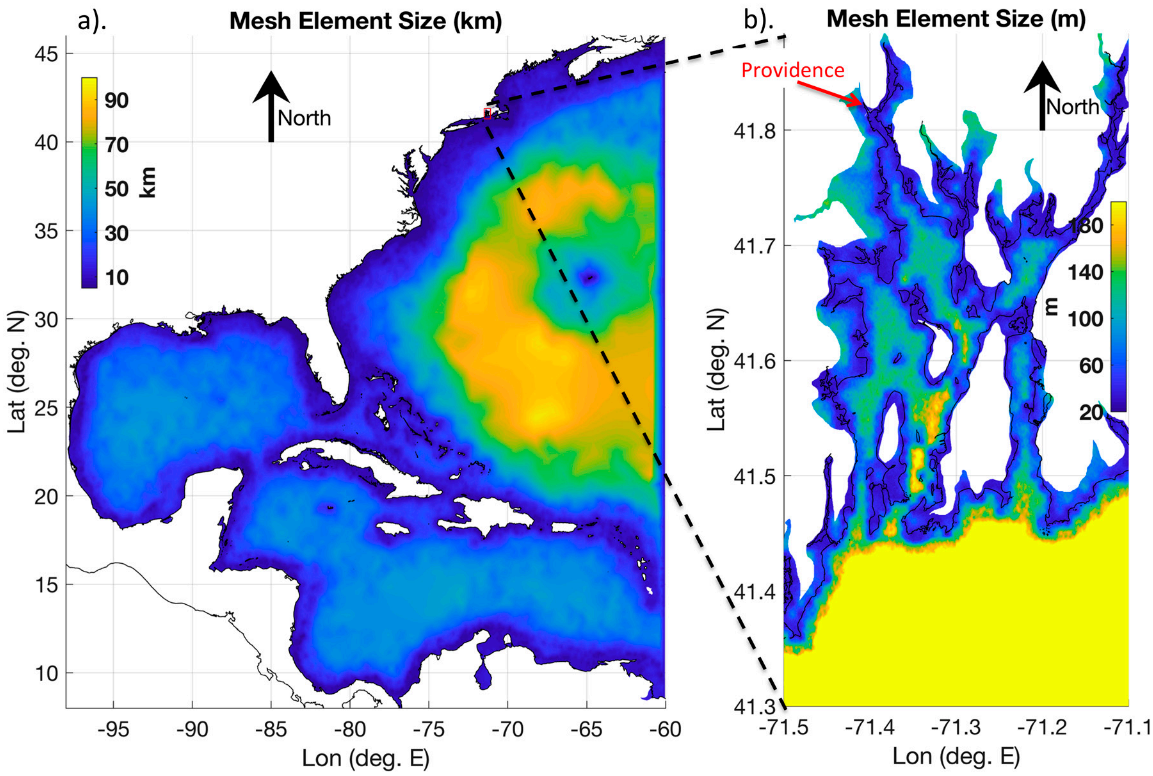

Figure 1. ADvanced CIRCulation (ADCIRC) mesh element size for (**a**) full domain in kilometers, and (**b**) Narragansett Bay (Rhode Island) region in meters.

The extensive damage to Providence from these hurricanes spurred the construction of the Fox Point Hurricane Barrier (FPHB), which was completed in 1966. The FPHB is made up of several elements (Figure 2): three movable Tainter gates spanning the upper Providence River (the northern portion of Narragansett Bay), dikes to the east and the west of the river, vehicular gates allowing access through the eastern dike, and a pumping station designed to discharge runoff from upstream of the Barrier when the Tainter gates are closed (see Figures 1 and 3 for the location of the Barrier). The design height of the FPHB is 25 feet (7.62 m) above the (now superseded) NGVD29 vertical datum [1]. Using the National Oceanic and Atmospheric Administration's (NOAA) VDatum conversion tool (https://vdatum.noaa.gov), the elevation at the top of the barrier is 7.37 m above NAVD88.

Figure 2. The Fox Point Hurricane Barrier (FPHB) in Providence, RI (photo is courtesy of The Providence Journal).

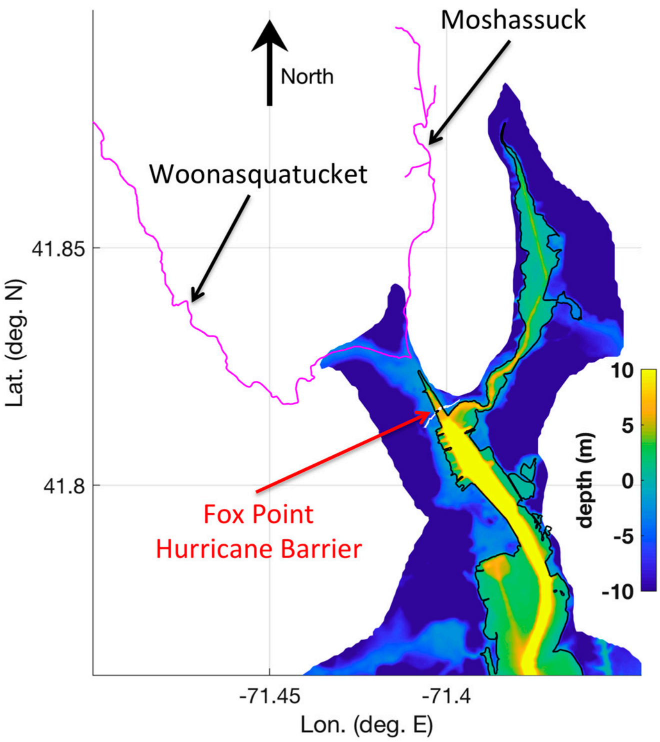

Figure 3. Mesh bathymetry in the Providence area at the northern end of Narragansett Bay. Land elevations are negative in this representation. The two rivers entering the domain to the north of the hurricane barrier are denoted by the magenta lines.

Since its construction, the FPHB has not faced a severe test, although it has been closed for several weaker tropical cyclones and winter storms. None of these events were severe enough to produce impacts that came close to compromising the Barrier. The purpose of this paper is to present results of storm surge and rainfall runoff modeling forced by an extreme yet plausible tropical cyclone strike in the southern New England region in order to raise awareness in the Rhode Island region and to evaluate the robustness of the FPHB. This hurricane, dubbed Rhody, is a hypothetical strong category three storm with characteristics similar to those of a number of historical hurricanes that have impacted the southern New England region. In addition to the strong category three Rhody, which is slightly stronger than any of the major hurricanes to strike the New England region during the last 100 years, we also present storm surge simulations for category four and five versions of Rhody. The purpose of this is to demonstrate, under present sea level, the limits of the FPHB in protecting the city of Providence.

There have been a number of related studies using coupled storm surge and wave models to examine the interaction of storm-driven surge with both natural and manmade barriers. The robustness of the Dutch Maeslant barrier to possible damage sustained during its operation was investigated by statistically estimating the recurrence time of instances in which water levels requiring the barrier's closure occurred twice within a certain time period (e.g., one month) [2]. For the three-barrier system protecting Venice, Italy, another study focused on determining the effect of various operation strategies (e.g., closure of only two barriers) on water levels in Venice Lagoon [3]. Storm surge modeling was also utilized in assessing the potential performance of proposed storm surge barriers in a Danish fjord [4] and at the mouth of the Mississippi River in the southern US [5]. Finally, several studies used a modeling approach to retrospectively evaluate the effects of barrier islands on storm surge elevation and water quality in the shallow back bays behind the barrier islands [6,7].

After discussing the methods used for generating the storm surge, the hurricane wind fields, and the river inflow, we discuss the synthetic storm, Hurricane Rhody. We then present the results of simulations of the storm surge resulting from the passage of an historical hurricane, Carol (1954), in order to demonstrate the skill of the modeling system. Subsequently, the storm surge and the river runoff impacts from Hurricane Rhody are presented.

2. Materials and Methods

2.1. Storm Surge Model

Storm surge impacts were computed using the ADvanced CIRCulation (ADCIRC) model (version 52) coupled with the Simulating Waves Nearshore (SWAN) model. ADCIRC is a finite element model that, in the two-dimensional mode employed here, solves for water level using the generalized wave continuity equation (GWCE) and for depth-averaged current using the shallow water momentum equations [8]. SWAN is a third-generation, phase-averaged wave model for simulating wind waves in coastal and open ocean regions [9]. ADCIRC and SWAN are coupled by passing the wave radiation stress computed from the SWAN wavefield to ADCIRC and passing the water levels, the currents, and the frictional parameters from ADCIRC to SWAN [10]. Both models are run on the same unstructured mesh using triangular elements.

The model mesh, consisting of 1,577,981 elements and 803,549 nodes, covers the northwestern Atlantic, the Caribbean Sea, and the Gulf of Mexico with an open boundary at longitude 60° W (Figure 1a). The mesh element size is coarse over the open ocean (50–100 km) and becomes finer over the continental shelf and near the coast. The element size in the Narragansett Bay region is less than 1 km and significantly less near the coast there, where elements are of the order of 30 m in size (Figure 1b). The mesh in the Rhode Island region extends upland to approximately the 10 m elevation contour to allow for overland flooding in the model. The model mesh includes the FPHB as a fixed weir (Figure 3) of height 7 m above mean sea level (MSL) using the results of the 2011 Rhode Island statewide LIDAR survey of the regional topography (http://www.rigis.org/pages/2011-statewide-lidar) rather than the design height referred to above.

The topography/bathymetry in the Rhode Island region was obtained from the Rhode Island Geographic Information System (RIGIS). The RIGIS statewide digital elevation model was derived from recent LIDAR surveys of land and historical bathymetric surveys, all converted to NAVD88 reference using NOAA's VDatum tool. Conversion to MSL reference was done using a spatially uniform value, taken to be the NAVD88-MSL difference of 0.093 m at the National Ocean Service (NOS) tide gauge at Newport, RI (NOS station 8452660). The bathymetry/topography for the southern New England region outside the RIGIS area were obtained from NOAA's 30 m resolution coastal DEM. Bathymetry in the remainder of the mesh was interpolated from historical soundings obtained from the National Ocean Service database (C. Fulcher, personal communication). Note that in the Narragansett Bay region, MSL is very close to NAVD88 (NAVD88-MSL = 0.07 m at Providence and 0.09 m at Newport), thus the difference in elevation between these datums is insignificant for this work.

ADCIRC was run in fully non-linear, two-dimensional mode with element wetting and drying enabled [11]. The GWCE solution was implemented using a spatially variable weighting parameter (τ_0), where τ_0 is specified as functions of the mesh element size and the local water depth [12]. Bottom friction was parameterized using a quadratic formulation where the drag coefficient (C_f) is a function of water depth via the Manning form, e.g., [13,14]:

$$C_f = \frac{gn^2}{\sqrt[3]{(H+\eta)}}, \tag{1}$$

where g is the gravitational acceleration, n is Manning's roughness, H is the undisturbed water depth, and η is the water surface elevation. A constant Manning roughness of 0.03 was specified, resulting in a depth dependent quadratic drag coefficient, as given by Equation (1). To avoid the extremely low values in deep water that would be provided by Equation (1) using constant n, a minimum drag coefficient of 3×10^{-3} was specified. This minimum value was achieved in water depth of approximately 25 m. The horizontal eddy viscosity was spatially uniform and set to 2 m^2/s.

The ADCIRC model was forced with winds at 10 m height and surface atmospheric pressure. The wind stress was computed from the wind speed at 10 m height using the quadratic drag law of Garratt [15]. The drag coefficient in the Garratt model increases linearly with 10 m wind speed. Because recent research suggests that the drag coefficient approaches a constant value or even decreases at higher wind speeds [16], we applied an upper limit of 2.8×10^{-3} to the drag coefficient, corresponding to wind speeds above 31 m/s.

At the eastern open boundary, located on the 60° W meridian, the model was forced with 8 tidal constituents (M_2, S_2, N_2, K_2, K_1, O_1, P_1, Q_1) interpolated from the TPXO7.2 global inverse model solution [17,18] (http://volkov.oce.orst.edu/tides/global.html). For all simulations, the tides were spun up by performing a run of 2–3 weeks in duration following a 2-day ramp-up period. An ADCIRC hotstart file containing the full model state written at the end of this spinup period was used as the initial condition for the hurricane forced simulations presented in this paper.

The FPHB is represented in ADCIRC as a natural internal barrier boundary consisting of a thin strip with paired nodes on the front and the back sides of the strip. If the model water surface elevation is higher than the barrier height and is not equal on both sides, water flow across the barrier occurs between paired nodes. The flow is computed using the formulae for flow across a broad crested weir [19], where the computation assumes either subcritical or supercritical flow depending on the relative heights of the water on either side of the barrier.

Inflows from the two rivers, Woonasquatucket and Moshassuck, flowing into upper Narragansett Bay north of the FPHB (see Figure 3) were implemented as normal flux boundary conditions at nodes along the upland boundary of the model mesh. The time varying normal flux was applied as an essential boundary condition. For simplicity, the combined volume flux from the rivers was applied as a normal flux boundary condition distributed over three nodes located where the Woonasquatucket River entered the model mesh (see Figure 3).

2.2. Wave Model

The SWAN model is a third generation, phase-averaged wave model that is based on shallow water wave physics. It solves the wave action equation for the wave frequency–direction spectrum using an implicit numerical scheme [9]. SWAN operates on the same unstructured mesh as is utilized by ADCIRC, which facilitates the coupling between the two models and eliminates the inter-mesh interpolation errors that would arise from the use of separate meshes [10,20].

For our wave simulations, the frequency space was discretized into 40 bins ranging from 0.03 to 1.42 Hz with a logarithmic increment factor of 1.1, and direction space was discretized into 36 bins [21]. A first order upwind scheme in geographic space, the default SWAN setting, was used as the propagation scheme. For the wind input term and the whitecapping term, the Rogers et al. [22] improvement to the Komen [23] formulation was used. In the coupled ADCIRC-SWAN system utilized here, wind stress information was passed to SWAN from ADCIRC. The parameterization used for bottom friction was based on the eddy-viscosity model of Madsen et al. [24]. With the spatial Manning's roughness coefficient and the water depth values passed from the ADCIRC model, this option enabled the computation of spatially and temporally varying bottom friction in SWAN [25]. For depth-induced breaking in the surf zone, the Battjes and Janssen [26] parameterization with default settings was chosen.

The coupling between SWAN and ADCIRC enabled a varying water level as well as current in the wave model, which could modify the behavior of waves in shallow water by altering the bottom friction, the depth-induced breaking, and the wave–current interaction. The wave impact on the storm surge was produced by the wave-induced force, the spatial gradient of the radiation stress, which was calculated from the SWAN-simulated wave spectrum. The ADCIRC/SWAN coupling was achieved by exchanging the above quantities every 600 s. It should be noted that the wave effects computed by the coupled SWAN/ADCIRC models were limited to wave setup arising from the radiation stress. Wave runup and wave overtopping of the FPHB, both of which could contribute to local flooding, were not simulated in the phase-averaged SWAN model.

2.3. River Runoff Model

The hydrological model, the Precipitation-Runoff Modeling System (PRMS), is a deterministic, distributed-parameter, physical process-based modeling system developed by the United States Geological Survey (USGS) to evaluate the response of various combinations of climate and land use on stream flow and general watershed hydrology [27]. PRMS's modular design allows users to selectively couple the modules in the module library or even to establish a self-design model. It has been widely applied in the research of rainfall-runoff modeling and has been demonstrated to be a reliable hydrological model. The model simulates the hydrologic processes of a watershed using a series of reservoirs that represent volumes of finite or infinite capacity. The PRMS model was applied to the simulation of rainfall runoff in the Taunton River Basin in Massachusetts and Rhode Island by Teng et al. [28] and showed good agreement with observations of stream flow during a storm event in 2010. Teng et al. [29] also investigated interactions between rainfall runoff and storm surge in Rhode Island's Woonasquatucket River.

2.4. Hurricane Wind and Rainfall Models

When hurricanes make landfall, the increased surface roughness of the land relative to that of the ocean produces changes in the spatial structure of the near-surface winds that are not captured by simple parametric models of hurricane winds. In order to account for these effects, the wind forcing fields for the storm surge simulations presented here were derived from a model of the hurricane boundary layer (HBL). The governing equations for the mean wind components were similar to those described in Gao and Ginis [30] but modified for a Cartesian coordinate system. The HBL model incorporated high vertical (30 m) and horizontal (1 km) resolutions combined with high-resolution information about topography and land use. At the upper boundary, the mean wind was assumed to be under the gradient wind balance. The spatial distribution of the gradient wind, Vg, was prescribed, and the pressure gradient force derived from the gradient balance equation was assumed vertically uniform. The turbulent viscosity was parameterized using a first-order scheme, e.g., [31], which was a function of the gradient Richardson number, the local strain rate, and a mixing length computed using the Blackadar form [32]. The Richardson number was computed using an imposed vertical profile of temperature that was constant in time [30]. At the lower boundary of the atmosphere, Monin–Obukhov similarity theory was used, where the roughness length over the ocean was parameterized as a function of wind speed [33] and over land as a function of land cover (https://landcover.usgs.gov/global_climatology.php).

The spatial distribution of the gradient wind, Vg, was derived from a parametric (vortex) model of hurricane winds driven by hurricane track and intensity parameters from the Tropical Cyclone Vitals Database (TCVitals) [34]. The parametric wind distribution was based on interpolation of the radial wind profiles derived from the TCVitals, as in the NOAA operational Hurricane Weather Research and Forecasting (HWRF) model [35].

Estimates of hurricane rainfall were derived from a rainfall climatology and persistence (R-CLIPER) model by Tuleya et al. [36]. This statistical, parametric model based on satellite-derived tropical cyclone rainfall observations assumed a symmetric rainfall distribution along the storm track. The rainfall distribution was parameterized as a function of storm intensity and size [36].

2.5. Hurricane Rhody

Hurricane Rhody is a hypothetical yet plausible hurricane scenario created to simulate the effects of a high-impact storm on the Rhode Island coast in order to provide state and local agencies with better understanding of the hazards associated with extreme hurricanes. The characteristics of the hurricane were not arbitrarily chosen but were based on those of several historical storms that have impacted the region. This ensures that, although it is artificial, Rhody is a potentially realizable storm for the region.

The storm forms near the Bahamas and propagates northward close to the US east coast. Similar to Hurricane Carol (1954), it tracks close to the coast, but it travels much more rapidly than Carol, moving at a rapid forward speed much like the 1938 New England Hurricane (Figure 4). The storm makes its initial landfall as a strong category 3 hurricane, with the eye crossing eastern Long Island and then eastern Connecticut (Figure 4) to the west of Rhode Island, a track that results in the most severe impacts in the Rhode Island region. After the first landfall, the hurricane slows and executes a loop, similar to the behavior of Hurricane Esther (1961), with the eye passing over Boston and then east and south of Cape Cod (Figure 4). It finally makes a second landfall, again to the west of Rhode Island, this time as a weaker, slower moving category 2 storm producing very heavy rainfall.

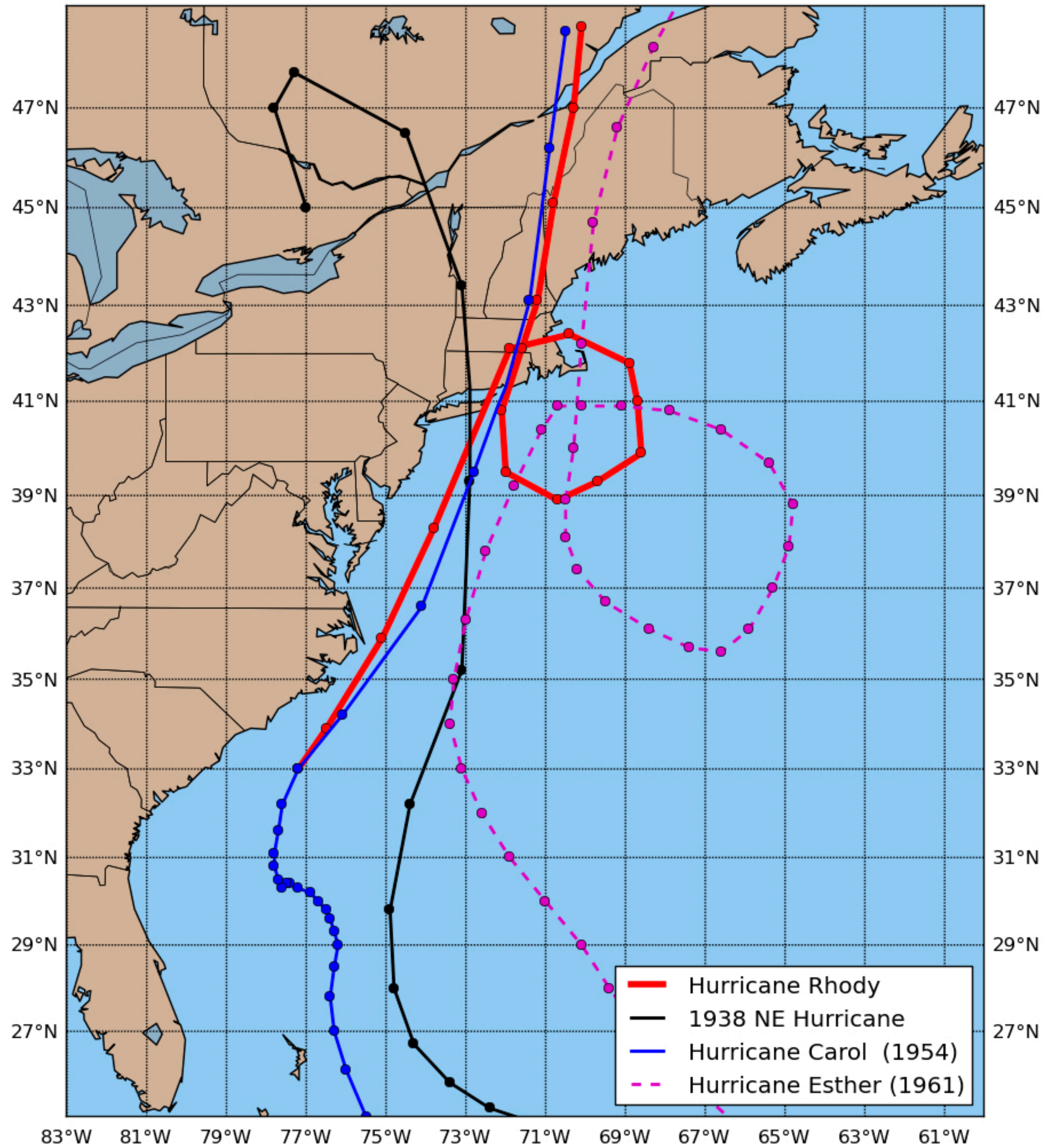

Figure 4. Track of Hurricane Rhody and those of three historical hurricanes whose characteristics were used as the basis for Rhody. The dots on the tracklines represent the storm positions at 12-h intervals.

Maps of wind speed magnitude at intervals of 6 h during a time period bracketing the first landfall are shown in Figure 5. The storm approaches New England with a forward speed of approximately 20 m/s (39 knots) with maximum wind speed of approximately 57 m/s at landfall (Figure 5a,b). At landfall (Figure 5b), the effect of land is apparent in the large reduction in wind speed over the northern half of the storm. Six hours after landfall (Figure 5c), the storm slows considerably, and over the next six hours (Figure 5d), it starts to move slowly to the south, the beginning of the loop that will eventually bring a second landfall.

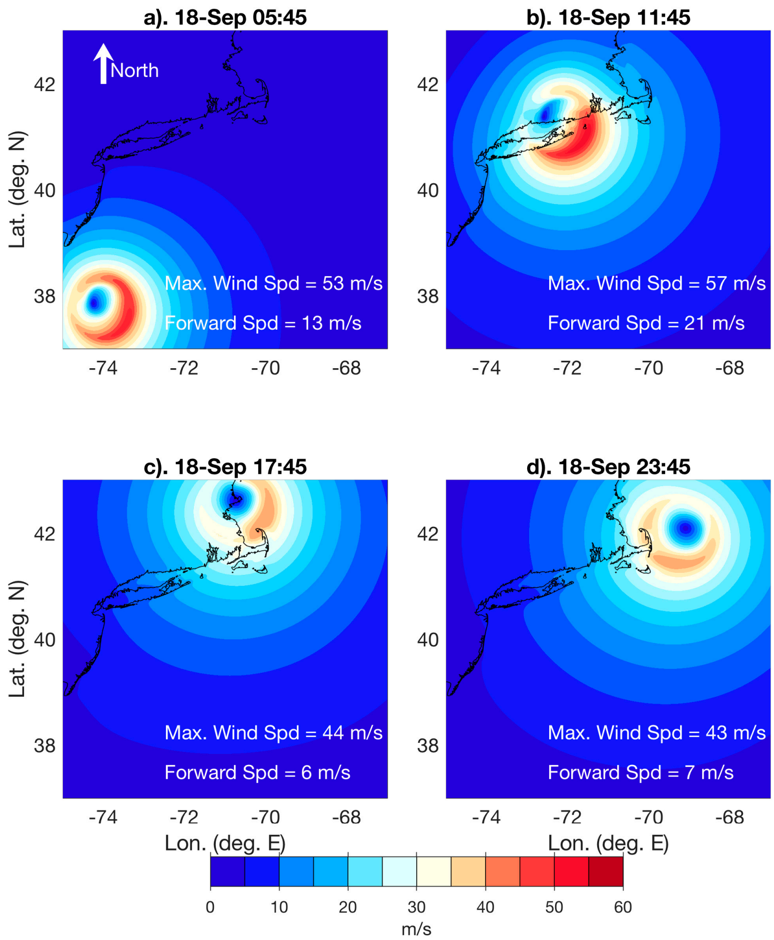

Figure 5. Wind speed at 10 m height for Hurricane Rhody at 6-h intervals during the period in which the first landfall occurs. (**a**) Approximately 6 h prior to landfall, (**b**) just after landfall on the mainland, (**c**,**d**) during the period when the storm slows and begins to execute the loop to the south.

In addition to the base Rhody case, we also created stronger versions of Rhody by scaling up the wind speeds such that the storm is of category 4 or 5 strength at landfall. The storm track and the forward speed are unchanged in these scenarios.

3. Results

3.1. Simulation of a Historical Hurricane

We first present simulations of a historical hurricane, Hurricane Carol, which impacted the Rhode Island region. Predicted water surface elevations are compared with the limited observations that were available from this storm in order to demonstrate the general performance of the model in simulating hurricane-forced storm surge.

Hurricane Carol struck the southern New England coast in 1954. On 31 August, the hurricane reached category three status just prior to making landfall at Point O'Woods, Long Island, NY. The storm quickly crossed the island and made a second landfall at Old Saybrook, CT. Sustained winds between 80–100 mph were experienced over eastern Connecticut, all of Rhode Island, and nearly all of eastern Massachusetts. A gust of 135 mph was recorded at Block Island, RI—the highest ever recorded at that location [37]. In addition to strong winds, Hurricane Carol also produced a very high storm surge, the highest of which was experienced in Narragansett Bay, submerging a quarter of the downtown Providence, RI area. Because Carol struck the region prior to the construction of the FPHB, we present a simulation on a model mesh without the barrier present. Limited observations were available for this time period—measurements of surface elevation at the NOS Newport tide gauge (obtained from NOAA/NOS) as well as measurements at South Street Station in Providence, close to the location of the present-day Providence tide gauge. The latter observations covering the storm surge period only were obtained from a NOAA report [37]. The water surface elevations at Providence, referenced to Mean Lower Low Water (MLLW) in the report [37], were converted to be relative to MSL (1960–1978 epoch) using datum information from the NOAA/NOS Providence station (8454000).

The Hurricane Carol storm surge simulated by ADCIRC/SWAN exhibits a high degree of spatial variability in Narragansett Bay. Maximum water surface elevation (relative to MSL) during the storm is approximately 3 m along the coast south of Narragansett Bay, decreasing to about 2.5 m in the lower portion of the Bay near Newport and then increasing northward to around 5 m in northern Narragansett Bay (Figure 6). This pattern is broadly consistent with a map of high water marks from Hurricane Carol presented in a US Weather Service report [38]. There is extensive flooding of land areas, especially in the northern Bay, but also in other low-lying areas around the region. Because the FPHB is not present, there is extensive flooding in Providence, as recorded during the actual storm.

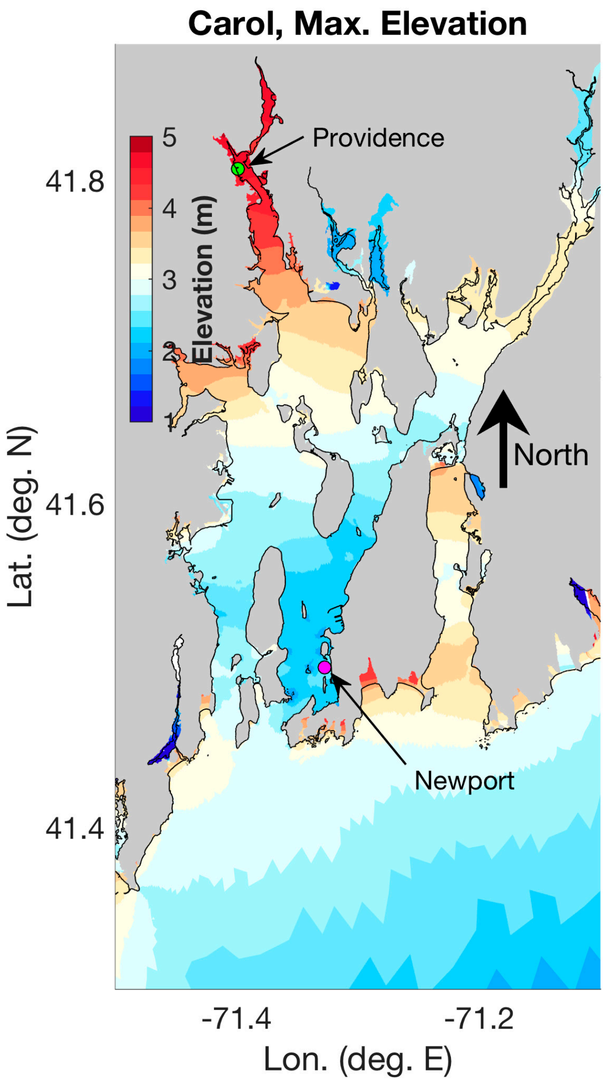

Figure 6. Simulated [ADCIRC/Simulating Waves Nearshore (SWAN)] maximum surface elevation for Hurricane Carol (1954) in the Narragansett Bay region with forcing from the hurricane boundary layer model. The mesh does not include the Fox Point Hurricane Barrier (FPHB), as this was not present at that time. The black line represents the coastline, and colored areas shoreward of the coastline represent areas experiencing overland flooding. The green and the magenta circles denote, respectively, the locations of the Providence and the Newport tide gauges.

Comparison of the model and the observed time series of water surface elevation at Providence and Newport (denoted by the green and magenta circles in Figure 6) show that the model captures the maximum surge water level at both sites quite well (Figure 7). However, the model storm surge duration is much shorter than the observed surge duration. It is possible that the shorter surge duration in the model could result in underestimation of the surge height in small embayments and valleys with narrow connections to the main Bay.

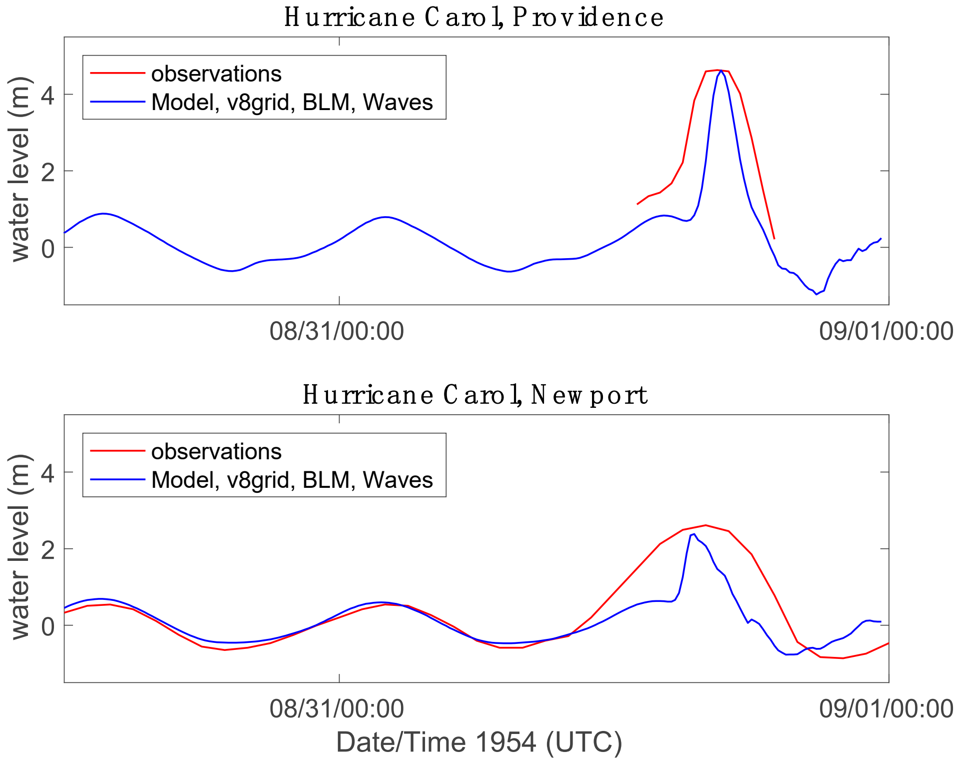

Figure 7. Time series comparison of model and observed water levels during Hurricane Carol at Providence (**top**) and Newport (**bottom**).

The shorter duration storm surge in the model could result from deficiencies in the specified wind forcing, where it is likely that the modeled wind does not adequately capture the far-field (far from the center) wind arising from larger scale meteorological processes. It is also possible that the poorly modeled forerunner surge [39] is due to unrealistically large bottom friction on the adjacent continental shelf that reduces the along-shelf wind driven velocity and the associated geostrophic setup. This possibility was tested by rerunning the Carol simulation but with the minimum drag coefficient set to 1×10^{-3} (compared to the value of 3×10^{-3} used for the base simulation). The results (not shown) indicate that this reduction leads to an insignificant increase in the surge height prior to the arrival of the main surge and no increase in the duration of the storm surge.

3.2. Hurricane Rhody Simulations

Because our aim is to raise local awareness of the potential catastrophic impacts of a major hurricane strike in southern New England, we selected the time period in which to embed Rhody such that its impacts were maximized. A spring tide period occurring in September 2016 was selected as the simulation time period. The start time of the Rhody simulation was selected such that the storm surge at Providence (at the northern end of Narragansett Bay) following the first landfall would occur at the time of astronomical high tide. With these assumptions, the Rhody storm surge simulation was performed (after a 15 day spin-up with no wind forcing) over a three day period commencing at 01:15 UTC on 18 September 2016.

3.2.1. Effect of Hurricane Barrier

The effects of a Rhody category three simulation on a mesh without the FPHB and with no river inflow are presented first in order to show the regional storm surge response to a hurricane of this magnitude. Figure 8, depicting the maximum water surface elevation (which occurs during the first landfall), shows the spatial variability associated with storm surge response in Narragansett Bay. Storm surge elevations range from minimum elevations above MSL of approximately 2–3 m in the lower Bay around Newport to roughly 6 m in the far northern reaches of the Bay (northeast of Providence). The surge in Providence is approximately 5.5 m, and extensive overland flooding occurs there and elsewhere around the Bay. Time series of surface elevation (Figure 9) indicate that the storm surge during the first landfall (on 18 September) is significantly higher than during the second landfall (on 20 September). After the first landfall, on 19 September, when the storm center is located northeast of Narragansett Bay, water surface elevations in the Bay drop significantly below the normal low tide level in response to strong winds from the north (Figure 9).

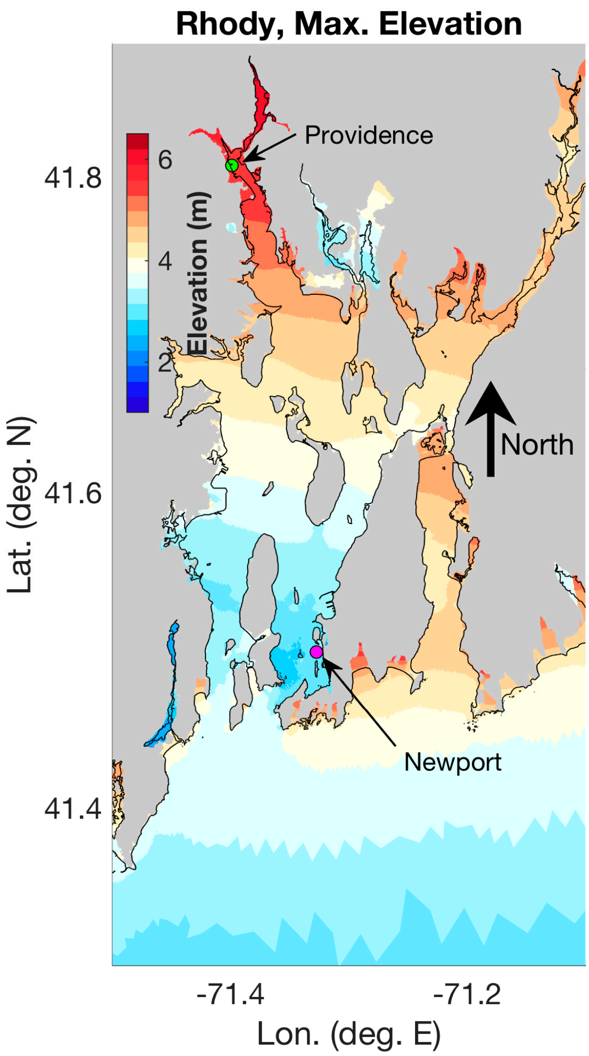

Figure 8. Simulated (ADCIRC/SWAN) maximum surface elevation for the synthetic storm Hurricane Rhody in the Narragansett Bay region on a mesh that does not include the FPHB and without river inflows. The black line represents the coastline, and colored areas shoreward of the coastline represent areas experiencing overland flooding. The green and the magenta circles denote, respectively, the locations of the Providence and the Newport tide gauges.

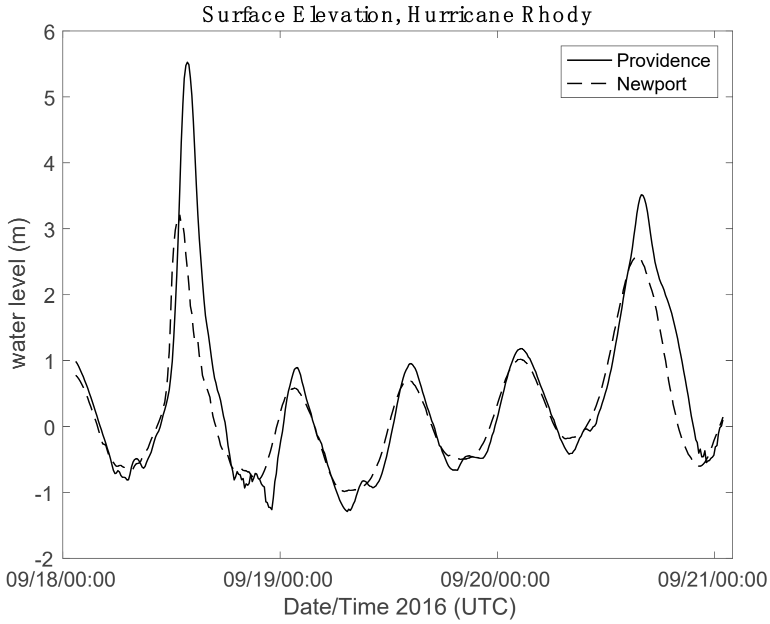

Figure 9. Time series of model water surface elevation during Hurricane Rhody at Providence and Newport. The model grid does not include the FPHB in this case, and river inflows are not simulated.

The ADCIRC/SWAN simulation with Rhody category three forcing on a mesh that includes the FPHB shows that flooding in downtown Providence (north of the Barrier) is prevented by the Barrier (Figure 10). From Figure 9, it is apparent that the storm surge in Providence during the first landfall of Rhody reaches 5.5 m above MSL, significantly below the 7 m height of the FPHB. This indicates that the FPHB will be effective in protecting downtown Providence under present sea level conditions and a strong category three hurricane. Not surprisingly, due to the fact that the area of the flood plain north of the Barrier is small, maximum storm surge elevations south of the Barrier are essentially unaffected by its presence (Figure 10).

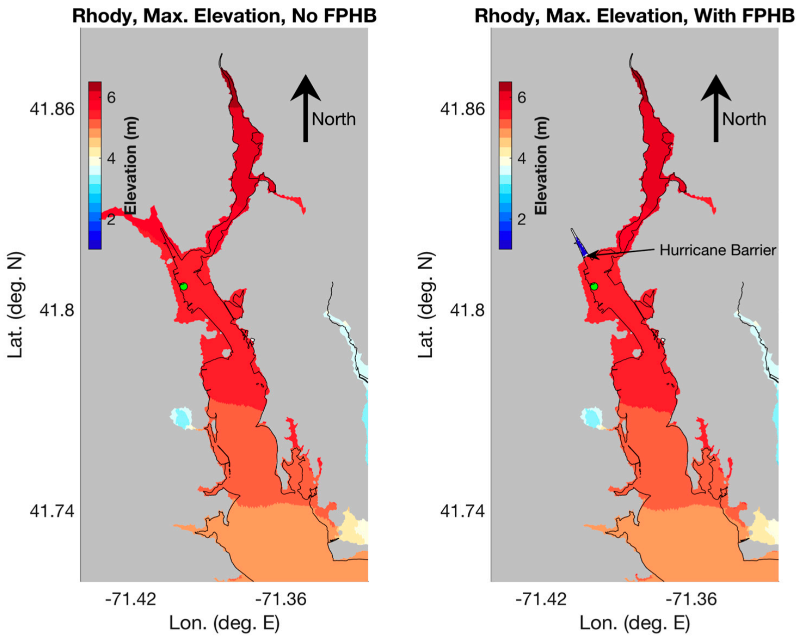

Figure 10. Simulated (ADCIRC/SWAN) maximum surface elevation for the synthetic storm Hurricane Rhody in the Narragansett Bay region comparing results from a mesh that does not include the FPHB (**left**) and a mesh that includes the FPHB (**right**). The simulations do not include river inflows. The black line represents the coastline, and colored areas shoreward of the coastline represent areas experiencing overland flooding. The green circle denotes the location of the Providence tide gauge.

3.2.2. How Robust is the Fox Point Hurricane Barrier?

The results presented above show that the FPHB is effective in protecting the area north of the Barrier from storm surge during a strong category three hurricane. A key question for the city of Providence is what magnitude of hurricane could potentially overflow the FPHB (neglecting, as mentioned above, wave effects)? To answer this question, a series of storm surge model simulations were performed with forcing from scaled-up versions of the Rhody wind field. The track, the forward speed, and the size of the storm remained constant, with only the wind speeds increased. The strength of the hurricane was quantified by the maximum wind speed at the time of its mainland landfall. In this way, simulations of category four and five versions of Rhody were performed in addition to the base category three version. The results show that the maximum surge increases as an approximately linear function of maximum wind speed (Figure 11). The maximum storm surge at Providence reaches the 7 m height of the FPHB under forcing from a weak category five hurricane.

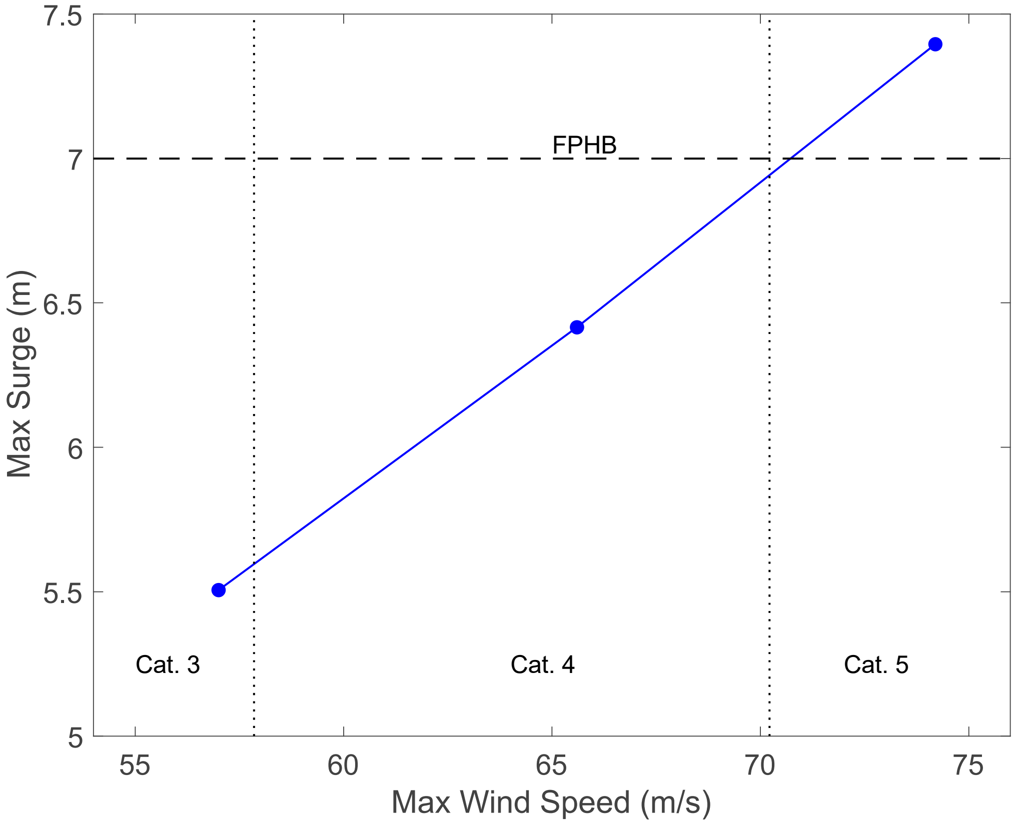

Figure 11. Maximum storm surge elevation at Providence [relative to mean sea level (MSL) versus maximum wind speed at hurricane landfall from simulations with varying strength Rhody forcing. The approximate elevation of the FPHB is shown by the horizontal dashed line. The vertical dotted lines denote the boundaries between Saffir–Simpson hurricane wind scale categories 3–5.

3.2.3. Effect of River Inflow

The large hurricane-forced storm surge during an extreme hurricane such as Rhody will likely be accompanied by massive regional power outages. Unless emergency power to the FPHB is available, the pumps that are designed to discharge river runoff from north of the Barrier will not be operable. This suggests that the area north of the FPHB may be susceptible to riverine flooding depending on the amount of rainfall during the hurricane. This possibility motivated the simulation of Hurricane Rhody impacts with the FPHB closed and with river inflows from the two rivers entering Narragansett Bay north of the Barrier.

Parameterized rainfall from Rhody using the R-CLIPER model produced an accumulated 4.2 inches of rain on 18 September, 5.4 inches on 19 September, and 9.8 inches on 20 September. The combined discharge of the Woonasquatucket and the Moshassuck rivers, simulated by the PRMS model, is shown in Figure 12 (top). This discharge was imposed as a normal flow boundary condition at three ADCIRC mesh boundary nodes in the Woonasquatucket valley. Water surface elevation at a location just north of the FPHB (red dot in Figure 13) increases slowly until the first landfall of Rhody, when the elevation fluctuates slightly due to the effect of the hurricane wind stress on the water within the impoundment north of the FPHB (Figure 12, bottom). After this time, the elevation north of the FPHB slowly increases as the area fills up with river discharge, and eventually (late on 20 September) water begins spilling over the Barrier, after which time the elevation remains constant at just over 7 m.

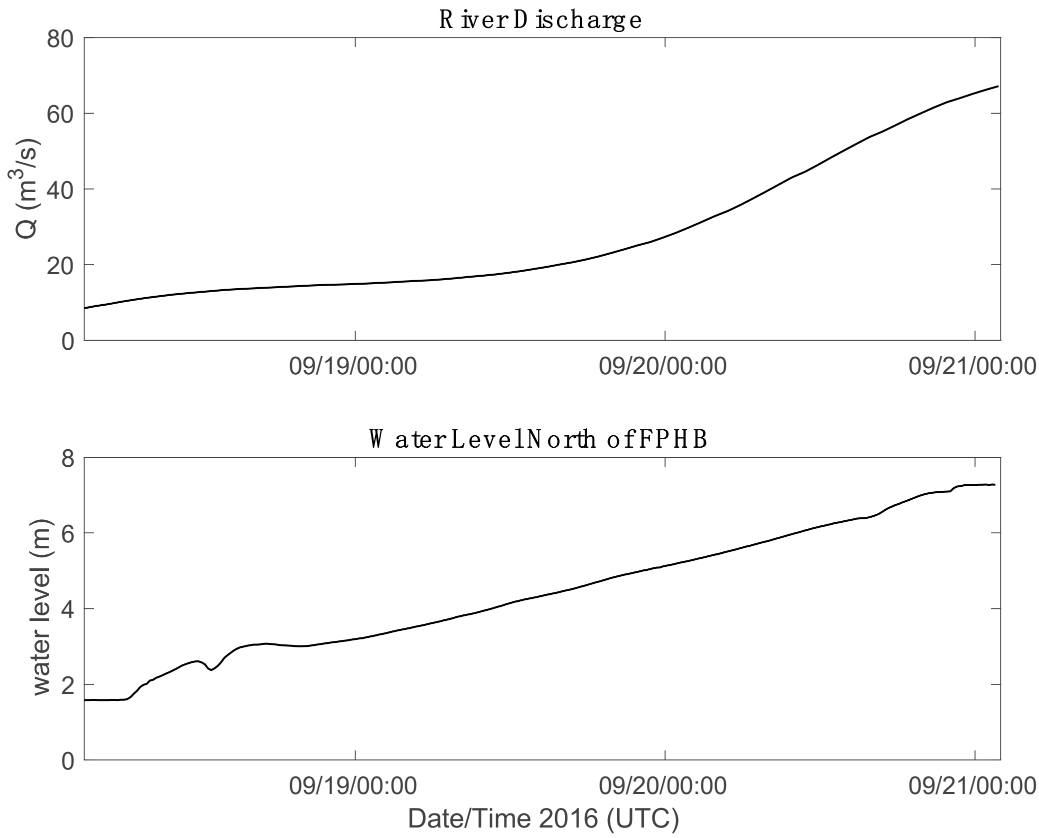

Figure 12. Combined (Woonasquatucket and Moshassuck Rivers) river discharge during hurricane Rhody computed from the PRMS model and applied as inflow forcing in ADCIRC/SWAN (top). The model water level just north of the (closed) FPHB is shown in the bottom plot.

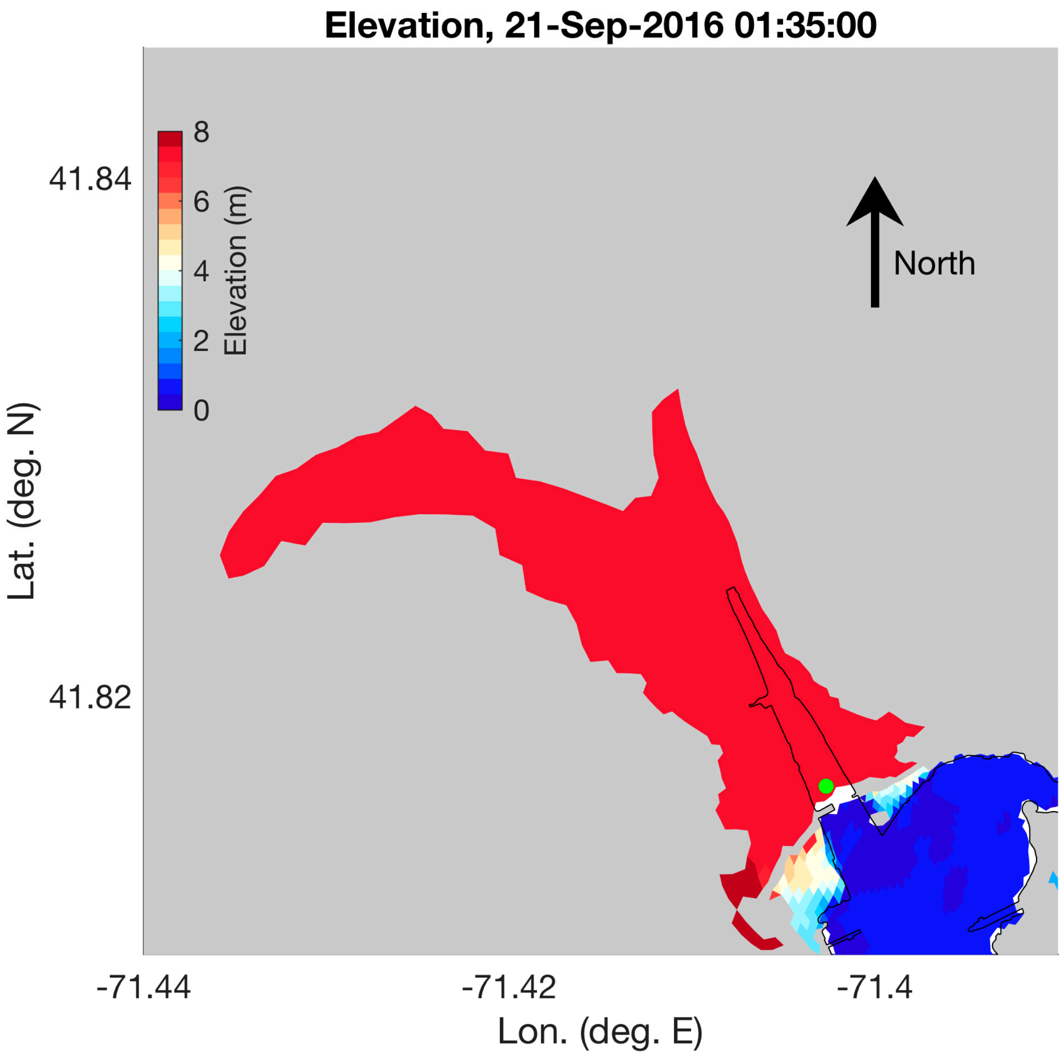

Figure 13. Water surface elevation in the Providence area at the end of the Rhody simulation including river discharge and the presence of the FPHB. The coastline is represented by the black line, and colored areas shoreward of the coastline represent areas experiencing overland flooding. The green dot is the location north of the FPHB at which a time series of surface elevation is shown in Figure 12 (bottom).

The spatial extent of the flooding resulting from Rhody rainfall at the end of the ADCIRC/SWAN simulation is shown in Figure 13. The elevation is approximately uniform everywhere north of the FPHB, and extensive areas in Providence are flooded. Although at this time storm surge flooding south of the barrier is not present, the effects of water flowing south across the barrier are seen in Figure 13 as the intermediate heights between the barrier and the shoreline south of the barrier.

3.2.4. Utilizing Hurricane Rhody Modeling for Improving Hurricane Preparedness

The catastrophic effects of rainfall from Hurricane Harvey in 2017 serve as a stark reminder that hurricanes may do damage through means that are not anticipated by the public or emergency managers and that may be very different from previously experienced storms. Through the use of high-resolution modeling, we can anticipate the possibility and the consequences of low probability but potentially catastrophic events. Our simulations of a hypothetical Hurricane Rhody illustrate the importance of considering the combined coastal and inland flooding. Southern New England is especially vulnerable to inland flooding, since the rivers are relatively short, and it is more likely that high river discharge resulting from hurricane rain will coincide with the storm surge.

The Hurricane Rhody scenario was used by Rhode Island Emergency Management Agency (RIEMA) and the FEMA Emergency Management Institute (EMI) to conduct an Integrated Emergency Management Course (IEMC) as part of a statewide preparedness exercise on June 19–22, 2017. The four-day exercise focused on the response to Hurricane Rhody while identifying key actions taken before, during, and after a hurricane. Outcomes from the course provided federal, state, and local decision makers with an opportunity to enhance overall preparedness while actively testing modeling outputs during various parts of the course. Figure 14 illustrates a three-dimensional (3-D) visualization of inundation effects in downtown Providence after the second Hurricane Rhody landfall that was used during the training course. Visualization tools such as these provide specific actionable outputs that are relevant to emergency and facility managers and can help decision makers to better prepare coastal communities for future risks during extreme weather events.

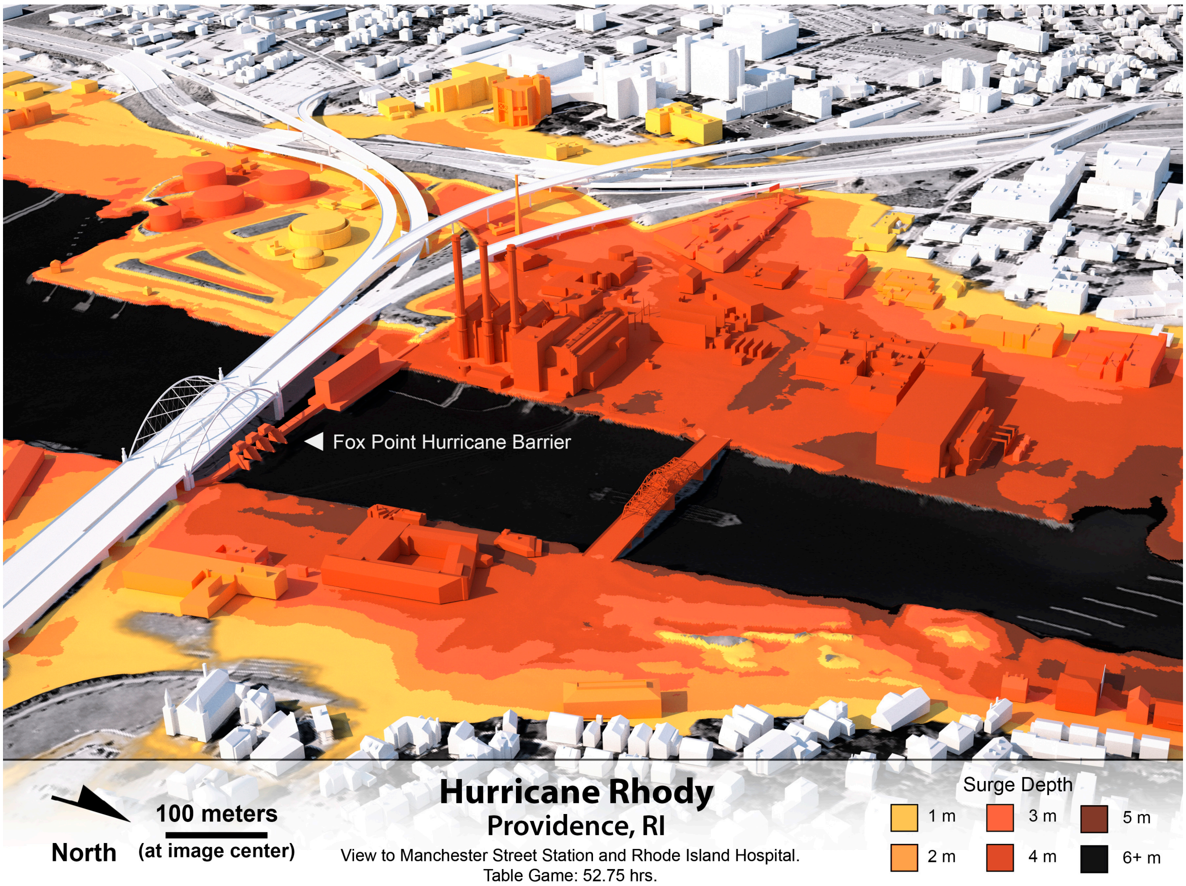

Figure 14. A three-dimensional (3-D) visualization of inundation effects in Providence, RI during the hypothetical Hurricane Rhody after its second landfall. The rivers enter the region from the right, and Narragansett Bay proper lies to the left.

4. Discussion

The simulated effects of the hypothetical Hurricane Rhody presented here represent the worst-case scenario due to the imposed timing of the landfall. The wave/storm surge simulation was set within an oceanic spring tide period, and the first landfall was timed such that the maximum surge occurred at high tide. At the NOAA/NOS Providence tide gauge during the September 2016 spring tide period, the predicted tidal range is approximately 2 m (https://tidesandcurrents.noaa.gov/waterlevels.html?id=8454000). This indicates that a change in the timing of landfall by 6.2 h (one half the period of the dominant M_2 tidal constituent) would result in total water level at the time of maximum storm surge approximately 2 m below the levels presented in this study. This indicates that storm surge impacts in the Providence region are strongly dependent on the timing of the wind-driven storm surge.

Comparison of simulations with and without the FPHB indicates that the Barrier is effective in mitigating the effects of all but the most extreme storm surge scenarios. Even though the Barrier is overflowed by the category five Rhody surge occurring at high tide, the area of flooding in Providence north of the Barrier is much reduced compared to the simulation without the FPHB (not shown). Furthermore, the category three results shown in Figure 10 indicate that the effects of the FPHB in the region outside the protected area in Providence are negligible. Differences in maximum surge between Rhody simulations with and without the FPHB are less than 0.15 m (not shown), an insignificant difference in comparison to the 5–7 m storm surge. This was not unexpected, since the area north of the FPHB is small in comparison to the area of Narragansett Bay.

The storm surge simulations with varying strength Hurricane Rhody forcing show that, under present sea level, the FPHB should be robust in protecting downtown Providence for storms of category four strength and below. Because hurricanes approaching New England from the south cross the mid-Atlantic Bight continental shelf, which has very cold bottom water during late spring through autumn [40], they tend to weaken prior to landfall, as this so-called Cold Pool is mixed vertically, thus reducing the sea surface temperature [41]. Thus, the likelihood of occurrence of a category five hurricane would appear to be low under present climatic conditions. However, under a warming climate, if the mid-Atlantic Bight Cold Pool were to warm, its capability to weaken hurricanes due to sea surface cooling would be reduced, thus increasing the likelihood of an extreme hurricane strike on southern New England.

The simulated rainfall/runoff impacts in Providence from Hurricane Rhody are predicated on the closure of the FPHB throughout the three day event due to the large-scale power outages expected in a severe hurricane that could preclude the opening of the Barrier after the first landfall. If power is unavailable after the first landfall, the assumption is that the Barrier's pumps would be inoperable as well. Clearly, if backup power is available, either the Barrier's gates could be raised after the first landfall, or the Barrier's pumps could be operated to move water across the closed Barrier. In either of these situations, the riverine flooding that we simulated would be avoided entirely or strongly mitigated.

5. Conclusions

We used numerical simulations of storm surge and river runoff to demonstrate the potential impacts of a severe hurricane strike in the Narragansett Bay region. The hypothetical hurricane, Rhody, is a physically realizable storm with characteristics based on those of hurricanes making landfall in the area during the past 80 years. During its first landfall, Rhody is a strong category three storm, making it stronger than any historical storm impacting the region during the modern era. The regional impacts of Rhody are severe, with large areas around the periphery of Narragansett Bay flooded. Water levels due to wind-driven storm surge associated with the first landfall of Rhody reach 5.5 m (relative to mean sea level) at the head of Narragansett Bay in the area around Providence. The FPHB (7 m height) is not overflowed in this scenario and protects downtown Providence from flooding, such as what occurred during the 1938 hurricane and Hurricane Carol (1954). After the first landfall, the storm moves northeast and then executes a slow loop to the south that is followed by a second landfall in southern New England. The storm surge resulting from the (weaker) hurricane winds at this time is lower than that occurring during the first landfall. The major impact around the time of the second landfall arises due to the assumed closure of the FPHB and the inoperability of its pumps. The intense rainfall predicted to occur around the time of the second landfall produces extremely high discharge in the rivers entering Narragansett Bay above the FPHB, and this is shown to result in severe flooding in Providence. These results emphasize the need to ensure that, after a hurricane strike, either the Barrier can be opened or the Barrier's pumps can be operated to discharge the river inflow across the Barrier.

Simulations with forcing from varying strength versions of hurricane Rhody show that, under present sea level, the FPHB will not protect the downtown area of Providence from storm surge flooding resulting from a land-falling category five storm (maximum winds greater than 70 m/s). As sea level rises over the coming decades, the robustness of the FPHB will clearly be reduced, making the city of Providence more vulnerable to storm surge.

Author Contributions: Conceptualization, D.S.U. and I.G.; methodology, D.S.U., I.G., W.H., C.N., X.C., and P.S.; software, D.S.U., C.N., X.C., and P.S.; validation, D.S.U., I.G., W.H., X.C., and P.S.; formal analysis, D.S.U. and I.G.; investigation, D.S.U., W.H., C.N., and X.C.; resources, I.G.; data curation, D.S.U. and P.S.; writing—original draft preparation, D.S.U., I.G., W.H., and X.C.; writing—review and editing, D.S.U. and I.G.; visualization, D.S.U. and P.S.; supervision, I.G.; project administration, I.G.; funding acquisition, I.G.

Funding: This research was funded by the US Department of Homeland Security as a part of grant award 2015-ST-061-ND0001-01. The views and conclusions contained in this document are those of the authors and should not be interpreted as necessarily representing the official policies, either expressed or implied, of the US Department of Homeland Security.

Acknowledgments: We thank Rick Luettich and Crystal Fulcher for providing their EC95d ADCIRC mesh, which was used as the starting point for the locally refined meshes used in this study. The comments of two anonymous reviewers are appreciated. Their suggestions have significantly improved the paper.

Conflicts of Interest: The authors declare no conflict of interest. The funders had no role in the design of the study; in the collection, analyses, or interpretation of data; in the writing of the manuscript, or in the decision to publish the results.

References

1. Morang, A. Hurricane Barriers in New England and New Jersey: History and Status after Five Decades. *J. Coast. Res.* **2016**, *32*, 181–205. [CrossRef]
2. Van den Brink, H.W.; de Goederen, S. Recurrence intervals for the closure of the Dutch Maeslant surge barrier. *Ocean Sci.* **2017**, *13*, 691–701. [CrossRef]
3. Cavallaro, L.; Iuppa, C.; Foti, E. EEffect of partial use of Venice flood barriers. *J. Mar. Sci. Eng.* **2017**, *5*, 58. [CrossRef]
4. Norgaard, J.Q.H.; Bentzen, T.R.; Larsen, T.; Andersen, T.L.; Kvejborg, S. Influence of closing storm surge barrier on extreme water levels and water exchange; the Limfjord, Denmark. *Coast. Eng. J.* **2014**, *56*, 1–16. [CrossRef]
5. Van Ledden, M.; Lansen, J.; de Ridder, H.; Edge, B. Reconnaissance level study Mississippi storm surge barrier. *Coast. Eng. Proc.* **2012**, *1*. [CrossRef]
6. Bennett, V.C.C.; Mulligan, R.P.; Hapke, C.J. A numerical model investigation of the impacts of Hurricane Sandy on water level variability in Great South Bay, New York. *Cont. Shelf Res.* **2018**, *161*, 1–11. [CrossRef]
7. Miselis, J.L.; Andrews, B.D.; Nicholson, R.S.; Defne, Z.; Ganju, N.K.; Navoy, A. Evolution of Mid-Atlantic coastal and back-barrier estuary environments in response to a hurricane: Implications for barrier-estuary connectivity. *Estuar. Coasts* **2016**, *39*, 916. [CrossRef]
8. Luettich, R.; Westerink, J., Jr.; Scheffner, N.W. *ADCIRC: An Advanced Three-Dimensional Circulation Model for Shelves, Coasts, and Estuaries. Report 1. Theory and Methodology of ADCIRC-2DDI and ADCIRC-3DL*; Dredging Research Program Technical Report DRP-92-6; U.S. Army Engineers Waterways Experiment Station: Vicksburg, MS, USA, 1992; 137p.
9. Booij, N.; Ris, R.; Holthuijsen, L. A third generation wave model for coastal regions. I. model description and validation. *J. Geophys. Res.* **1999**, *104*, 7649–7666. [CrossRef]
10. Dietrich, J.; Zijlema, M.; Westerink, J.; Holthuijsen, L.; Dawson, C.; Luettich, R.A., Jr.; Jensen, R.; Smith, J.; Stelling, G.; Stone, G. Modeling hurricane waves and storm surge using integrally-coupled, scalable computations. *Coast. Eng.* **2011**, *58*, 45–65. [CrossRef]
11. Dietrich, J.C.; Kolar, R.L.; Luettich, R.A. Assessment of ADCIRC's wetting and drying algorithm. *Dev. Water Sci.* **2004**, *55*, 1767–1778. [CrossRef]
12. Westerink, J.J.; Luettich, R.A.; Feyen, J.C.; Atkinson, J.H.; Dawson, C.; Roberts, H.J.; Powell, M.D.; Dunion, J.P.; Kubatko, E.J.; Pourtaheri, H. A basin-to channel-scale unstructured grid hurricane storm surge model applied to southern Louisiana. *Mon. Weather Rev.* **2008**, *136*, 833–864. [CrossRef]
13. Bunya, S.; Dietrich, J.C.; Westerink, J.J.; Ebersole, B.A.; Smith, J.M.; Atkinson, J.H.; Jensen, R.; Resio, D.T.; Luettich, R.A.; Dawson, C.; et al. A high-resolution coupled riverine flow, tide, wind, wind wave, and storm surge model for southern Louisiana and Mississippi. Part I: Model development and validation. *Mon. Weather Rev.* **2010**, *138*, 345–377. [CrossRef]

14. Kerr, P.C.; Martyr, R.C.; Donahue, A.S.; Hope, M.E.; Westerink, J.J.; Luettich, R.A., Jr.; Kennedy, A.B.; Dietrich, J.C.; Dawson, C.; Westerink, H.J. U.S. IOOS coastal and ocean modeling testbed: Evaluation of tide, wave, and hurricane surge response sensitivities to mesh resolution and friction in the Gulf of Mexico. *J. Geophys. Res.* **2013**, *118*, 4633–4661. [CrossRef]
15. Garratt, J.R. Review of drag coefficients over oceans and continents. *Mon. Weather Rev.* **1977**, *105*, 915–929. [CrossRef]
16. Bryant, K.M.; Akbar, M. An exploration of wind stress calculation techniques in hurricane storm surge modeling. *J. Mar. Sci. Eng.* **2016**, *4*, 58. [CrossRef]
17. Egbert, G.D.; Bennett, A.F.; Foreman, M.G.G. TOPEX/POSEIDON tides estimated using a global inverse model. *J. Geophys. Res.* **1994**, *99*, 24821–24852. [CrossRef]
18. Egbert, G.D.; Erofeeva, S.Y. Efficient inverse modeling of barotropic ocean tides. *J. Atmos. Ocean. Technol.* **2002**, *19*, 183–204. [CrossRef]
19. Henderson, F.M. *Open Channel Flow*; MacMillan Company: Toronto, ON, Canada, 1966.
20. Zijlema, M. Computation of wind-wave spectra in coastal waters with SWAN on unstructured grids. *Coast. Eng.* **2009**, *57*, 267–277. [CrossRef]
21. Hope, M.E.; Westerink, J.J.; Kennedy, A.B.; Kerr, P.C.; Dietrich, J.C.; Dawson, C.; Bender, C.J.; Smith, J.M.; Jensen, R.E.; Zijlema, M.; et al. Hindcast and validation of Hurricane Ike (2008) waves, forerunner, and storm surge. *J. Geophys. Res.* **2013**, *118*, 4424–4460. [CrossRef]
22. Rogers, W.E.; Hwang, P.A.; Wang, D.W. Investigation of wave growth and decay in the SWAN model: Three regional-scale applications. *J. Phys. Oceanogr.* **2003**, *33*, 366–389. [CrossRef]
23. Komen, G.J.; Hasselmann, S.; Hasselmann, K. On the existence of a fully developed wind-sea spectrum. *J. Phys. Oceanogr.* **1984**, *14*, 1271–1285. [CrossRef]
24. Madsen, O.S.; Poon, Y.-K.; Graber, H.C. Spectral wave attenuation by bottom friction: Theory. *Coast. Eng.* **1988**, *1988*, 492–504. [CrossRef]
25. Dietrich, J.C.; Westerink, J.J.; Kennedy, A.B.; Smith, J.M.; Jensen, R.E.; Zijlema, M.; Holthuijsen, L.H.; Dawson, C.; Luettich, R.A.; Powell, M.D.; et al. Hurricane Gustav (2008) waves and storm surge: Hindcast, synoptic analysis, and validation in southern Louisiana. *Mon. Weather Rev.* **2011**, *139*, 2488–2522. [CrossRef]
26. Battjes, J.A.; Janssen, J.P.F.M. Energy loss and set-up due to breaking of random waves. *Coast. Eng.* **1978**, *1978*, 569–587.
27. Markstrom, S.L.; Regan, R.S.; Hay, L.E.; Viger, R.J.; Webb, R.M.T.; Payn, R.A.; LaFontaine, J.H. *PRMS-IV, the Precipitation-Runoff Modeling System*, Version 4; U.S. Geological Survey Techniques and Methods: Reston, VA, USA, 2015; Book 6, Chap B7; 158p. Available online: https://pubs.usgs.gov/tm/6b7/ (accessed on 2 November 2017).
28. Teng, F.; Huang, W.; Ginis, I. Hydrological modeling of storm-induced runoff and snowmelt in Taunton River Basin. *J. Nat. Hazards* **2018**, *91*, 179–199. [CrossRef]
29. Teng, F.; Huang, W.; Ginis, I.; Cai, Y. Characteristics of River Flood and Storm Surge Interactions in a Tidal River in Rhode Island, USA. *Procedia IUTAM* **2017**, *25*, 60–64. [CrossRef]
30. Gao, K.; Ginis, I. On the equilibrium-state roll vortices and their effects in the hurricane boundary layer. *J. Atmos. Sci.* **2016**, *73*, 1205–1221. [CrossRef]
31. Zhang, J.A.; Drennan, W.M. An observational study of vertical eddy diffusivity in the hurricane boundary layer. *J. Atmos. Sci.* **2012**, *69*, 3223–3236. [CrossRef]
32. Blackadar, A.K. The vertical distribution of wind and turbulent exchange in a neutral atmosphere. *J. Geophys. Res.* **1962**, *67*, 3095–3102. [CrossRef]
33. Moon, I.-J.; Ginis, I.; Hara, T.; Thomas, B. A physics-based parameterization of air-sea momentum flux at high wind speeds and its impact on hurricane intensity predictions. *Mon. Weather Rev.* **2007**, *135*, 2869–2878. [CrossRef]
34. Trahan, S.; Sparling, L. An analysis of NCEP tropical cyclone vitals and potential effects on forecasting models. *Weather Forecast.* **2012**, *27*, 744–756. [CrossRef]
35. Yablonsky, R.M.; Ginis, I.; Thomas, B.; Tallapragada, V.; Sheinin, D.; Bernardet, L. Description and analysis of the ocean component of NOAA's operational Hurricane Weather Research and Forecasting (HWRF) Model. *J. Atmos. Oceanic Technol.* **2015**, *32*, 144–163. [CrossRef]
36. Tuleya, R.E.; DeMaria, M.; Kuligowski, R.J. Evaluation of GFDL and simple statistical model rainfall forecasts for U. S. landfalling tropical storms. *Weather Forecast.* **2007**, *22*, 56–70. [CrossRef]

37. Vallee, D.R. *Rhode Island Hurricanes and Tropical Storms, a Fifty-Six Year Summary, 1936–1991*; NOAA Technical Memorandum NWS ER-86; National Weather Service Office: Providence, RI, USA, 1993; 62p.
38. Harris, D.L. *Characteristics of the Hurricane Storm Surge*; No. 48; United States Weather Bureau Technical Paper: Washington, DC, USA, 1963; 139p.
39. Kennedy, A.B.; Gravois, U.; Zachry, B.C.; Westerink, J.J.; Hope, M.E.; Dietrich, J.C.; Powell, M.D.; Cox, A.T.; Luettich, R.A., Jr.; Dean, R.G. Origin of the Hurricane Ike forerunner surge. *Geophys. Res. Lett.* **2011**, *38*, L08608. [CrossRef]
40. Houghton, R.W.; Schlitz, R.; Beardsley, R.C.; Butman, B.; Chamberlin, J.L. The Middle Atlantic Bight cold pool: Evolution of the temperature structure during summer 1979. *J. Phys. Oceanogr.* **1982**, *12*, 1019–1029. [CrossRef]
41. Glenn, S.M.; Miles, T.N.; Seroka, G.N.; Xu, Y.; Forney, R.K.; Yu, F.; Roarty, H.; Schofield, O.; Kohut, J. Stratified coastal ocean interactions with tropical cyclones. *Nat. Commun.* **2016**, *7*, 1–10. [CrossRef] [PubMed]